Title

ISOTOPE PRODUCTION CROSS SECTIONS FROM THE FRAGMENTATION OF 16O AND 12C AT RELATIVISTIC ENERGIES

Authors

Lindstrom, P.J.
Greiner, D.E.
Heckman, H.H.
et al.

Publication Date

1975-02-01

Submitted to Physical Review Letters

LBL-3650
Preprint c. 1

ISOTOPE PRODUCTION CROSS SECTIONS FROM THE FRAGMENTATION OF ^{16}O AND ^{12}C AT RELATIVISTIC ENERGIES

P. J. Lindstrom, D. E. Greiner, H. H. Heckman,
Bruce Cork, and F. S. Bieser

February, 1975

Prepared for the U. S. Atomic Energy Commission
under Contract W-7405-ENG-48

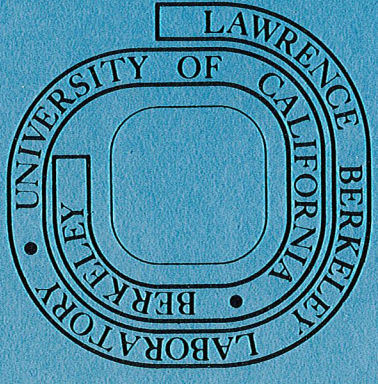

LBL-3650

ISOTOPE PRODUCTION CROSS SECTIONS FROM THE FRAGMENTATION OF ^{16}O AND ^{12}C AT RELATIVISTIC ENERGIES.*

P. J. Lindstrom, D. E. Greiner,† H. H. Heckman and Bruce Cork

Lawrence Berkeley Laboratory
University of California
Berkeley, California 94720 U.S.A.

and

F. S. Bieser

Space Sciences Laboratory
University of California
Berkeley, California 94720 U.S.A.

ABSTRACT

The 0-degree fragmentation products of ^{16}O and ^{12}C at 2.1 -GeV/n and ^{12}C at 1.05 -GeV/n have been measured for targets ranging from H to Pb. We present a total of 464 partial-production cross sections for 35 isotopes. The cross sections are energy independent and can be factored into beam-fragment and target terms. The target factor, $\gamma_T \propto A_T^{1/4}$, and other evidence, imply the isotopes are produced in peripheral interactions.

We have measured at the Bevatron the single-particle inclusive spectra of all isotope fragments of ^{16}O and ^{12}C at 2.10 GeV/n and of ^{12}C at 1.05 GeV/n. The targets were Be, CH_2, C, Al, Cu, Ag, and Pb. The hydrogen target data were obtained by CH_2-C subtraction. The measurements were limited to secondaries produced within a ±12.5 mr cone about 0-deg from the direction of the primary beam. Secondary momenta were limited to rigidities (pc/Ze) less than 9 GV. All secondaries with lifetimes greater than 10^{-8} seconds and production cross sections greater than 10μb were observed. The spectrometer system[1,2] resolved charge, mass, and momentum for all secondaries at any given spectrometer rigidity setting.

The observed longitudinal and transverse momentum spectra of the isotope fragments, when transformed to the projectile rest frame, have Gaussian distributions centered near 0-MeV/c, with standard deviations (S.D) ∿60-200 MeV/c. The cross sections presented in Table I were obtained by integrating these momentum distributions. Since the observed fragments were confined to a 12.5 mr cone, it was necessary to extrapolate the transverse momentum distributions to obtain total partial cross sections. Except for the $Z \leqslant 2$ fragments, the 12.5 mr region accounted for 70%-100% of the total cross sections. Both observed momentum systematics[2] and measured angular distributions in nuclear emulsion[3] give confidence in this extrapolation for $A \geqslant 2$ secondaries. The proton momentum distribution is non-Gaussian and no attempt was made to extrapolate this distribution to estimate total production cross sections. The cross sections are corrected for beam and secondary fragmentation in the targets, vacuum windows, and scintillators, as well as for interactions in the Si(Li) detectors. Corrections are made for focus, geometry, misalignment, and multiple

secondaries with the same rigidity. Focus, solid angle, and target-loss errors give a base 4-8% systematic error which is included in Table I [4] errors. The momentum distributions show the cross sections σ_{BT}^{F}, where beam B interacts with target T to produce fragment F, are measurements of fragments of the projectile, and not fragments of the target. No fragments were observed with velocities much less than beam velocity. No nucleon-pickup isotopes were observed. Between 30% (Pb target) and 90% (H target) of all beam charge is accounted for in Table I σ_{BT}^{F}. The missing charge is principally in large momentum transfer protons.

The σ_{BT}^{F}, for a hydrogen target, can be compared with cross sections of proton-nucleus interactions at high energies. At proton energies $\geq$ 600 MeV, 42 measured cross sections for 15 different secondaries have been compiled.[5,6] Comparing Table I data with the proton measurements, 24 are within 1 S.D., 9 are within 1-2 S.D., 7 are 2-3 S.D., and 2 are 3-4 S.D. The two cross section measurements 3-4 S.D. from our data are $p + {}^{16}O \rightarrow {}^{10}C + ---$ at T_p= 1 GeV and $p + {}^{16}O \rightarrow {}^{10}Be + ---$ at 600 MeV. Comparison of our results can also be made with the semi-empirical model by Silberberg and Tsao[8], which is based on the proton-nucleus data set mentioned above. We find the experimental values σ_{BT}^{F} above 1 mb listed in Table I are greater than those given by the Silberberg and Tsao model by an average of 22%, with a S.D. of 37%.

Target factorization is expected both from high energy phenomenology[9] and from an impulse approximation model of nuclear fragmentation.[10] We observe that the cross sections can be factored, $\sigma_{BT}^{F} = \gamma_{B}^{F} \gamma_{T}$, where γ_{B}^{F} depends on the projectile and fragment and γ_{T} is the target factor (Fig. 1). This result confirms, and significantly extends, the first experiments on the fragmentation of relativistic nuclei.[11] The exceptions to strict factorization are: 1) γ_{T}

for a hydrogen target has a weak dependence on the mass of fragment A_F, i.e., $\gamma_T(H) = 0.66 + 0.028\ A_F$; and 2) γ_T for single-nucleon stripping is enchanced for heavy targets. The cross sections for single-nucleon loss on the heavier targets include a component for Coulomb dissociation, via the giant dipole resonance, in the target's virtual photon field. The Coulomb dissociation part of the cross sections can be computed[12] and subtracted from the measured σ_{BT}^F. The resultant cross sections are consistent with the target factors given in Table I. The target factors fit the data with a confidence level of 0.6, and can be approximately fitted by the expression $\gamma_T = A_T^{1/4}$ or $\gamma_T \propto (A_B^{1/3} + A_T^{1/3} - 1.6)$. Both formulations for γ_T indicate the cross sections we observe are produced by peripheral interactions with the target. Neither formulation for γ_T explains the observed structure, however, particularly the result $\gamma_T(Be) > \gamma_T(C)$.

Although $A_T^{1/4}$ generally fits the observed data to within 10%, the confidence level for this hypothesis is less than 10^{-9}. An accurate fit to the target factor is obtained by the expression $\gamma_T = kt^n\ (r_T+b)$ where r_T is the measured half-density electric-charge radius and t is the measured charge skin thickness of the target.[13] The three fitted variables are: the exponent n = 0.5, b=3.0 fm, and normalizing constant k=0.26. This formula reproduces the structure in the mean target factor to an accuracy better than 2% and with a confidence level of 0.9, a great improvement over the $A^{1/4}$ hypothesis. Since σ_{BT}^F factors and the momenta distributions are target independent,[2] the partial differential cross sections factor -- a result expected by limiting fragmentation models. Whether γ_T contains beam-dependent terms, e.g., the sum of the radii of the beam and target nuclei, as suggested above, cannot be determined with the present data.

The energy dependence of isotope production can be examined by 1) comparing σ^F_{BT}, Table I, for the two ^{12}C-beam energies, and 2) comparing σ^F_{BT} with values from Ref. 5 & 6, measured at different energies. The carbon data for all fragments are energy independent between 1.05 and 2.10 GeV/n with a confidence level of 0.8. The error-weighted mean ratio σ^F_{BT} (2.10)/σ^F_{BT}(1.05) = 1.01 ± 0.01. We have already mentioned comparison of σ^F_{BT}, for both ^{12}C and ^{16}O projectiles with previously measured target data and the agreement was generally good for energies 600 MeV/n and above. Energy independence of σ^F_{BT}, above some energy threshold, is another result expected from high energy phenomenology. A comparison of σ^F_{BT} for the same fragments and targets but different beams, ^{16}O and ^{12}C, shows, in general, a weak beam dependence in the production cross sections of all fragments in common, as long as a charge-exchange reaction is not necessary. The ratio $\sigma^F_{BT}(^{16}O)/\sigma^F_{BT}(^{12}C)$=0.4-1.35, even though the individual cross sections vary over three orders of magnitude. It is noteworthy that more than 40% of the ratios are in the interval 1.0 ± 0.15.

Production cross sections for mirror nuclei should give insight into the mechanisms which produce the observed final state. A simple evaporation model would preferentially evaporate neutrons resulting in $\sigma_N/\sigma_P \leq 1$, where σ_N/σ_P is the ratio of the production cross sections for mirror fragments, neutron rich to proton rich, of the same beam and target. Likewise, if a neutron skin extends beyond the proton surface, a stripping process would also result in $\sigma_N/\sigma_P \leq 1$. We observe that, to the contrary, $1.0 < \sigma_N/\sigma_P < 4.1$, with most values of the ratio being in the interval 1.1 to 1.7. That $\sigma_N/\sigma_P > 1$ is indicative of the effects of the binding energy of the final state fragment. For example, inspection of the mass excess vs σ^F_{BT} for isobars shows the fragment with the lower mass excess has

the higher production cross section. This dominance of final state structure in σ_{BT}^{F} complicates the choice of any simple mechanism describing the interaction process.

The patterns observed in σ_{BT}^{F} and in the momentum distributions[2] indicate simplicity in the peripheral fragmentation process. Target factorization, energy independence, and small transverse momenta are observed features of σ_{BT}^{F} and directly relate to limiting fragmentation models. The $A_T^{\frac{1}{4}}$ behavior of the target factor and the inclusion of a charge skin-thickness term in the best fit for γ_T, along with small parallel momenta widths in the beam rest frame, imply the observed fragments are the result of peripheral interactions. Neutron rich enchancement of mirror-isotope cross sections, correlations in fragment binding energies, and a surprising degree of beam independence in σ_{BT}^{F} indicate a dominance of fragment nuclear structure in the production amplitudes.

We thank the Bevatron operations staff, under H. A. Grunder and R. J. Force, for their support and effort during this experiment. We commend E. E. Beleal, D. M. Jones and C. P. McParland for their computer programming efforts and data handling, and R. C. Zink for electronic component construction.

REFERENCES

*Work performed under auspices of the U.S. Atomic Energy Commission and the National Aeronautics and Space Administration Grant NGR 05-003-513.

†Dual appointment with U. C. Space Sciences Laboratory.

1. For spectrometer characteristics see D. E. Greiner, P. J. Lindstrom, F. S. Bieser, and H. H. Heckman, Nucl. Inst. and Methods, 116, 21 (1974).
2. D. E. Greiner, P. J. Lindstrom, H. H. Heckman, B. Cork, and F. S. Bieser, (submitted to Phys. Rev. Letters). LBL Report No. 3651, 1975.
3. H.H. Heckman, D.E. Greiner, P.J. Lindstrom, Hla Shwe, LBL Report No. 3656, 1975 (to be published).
4. The cross sections in Table I are available on computer cards.
5. R. Silberberg and C. H. Tsao, NRL Report No. 7593 (1973).
6. F. Yiou, G. Raisbeck, C. Perron, and P. Fontes, Conference papers, 13th International Cosmic Ray Conference, Denver, Colorado, 17-30 August 1973, Vol. I, Paper No. 251.
7. G. Raisbeck and F. Yiou, Conference papers, 13th International Cosmic Ray Conference, Denver, Colorado, 17-30 August 1973, Vol. I, Paper No. 253.
8. R. Silberberg and C. H. Tsao, Ap. J. Suppl, No. 220(I), 25, 315 (1973).
9. For a General review, see W. R. Frazer et. al., Rev. Mod. Phys. 44, 284 (1972).
10. J. V. Lepore and R. J. Riddell Jr., LBL 3086, 1974 (unpublished).
11. H. H. Heckman, D. E. Greiner, P. J. Lindstrom, and F. S. Bieser, Phys. Rev. Letters 28, 926 (1972).
12. X. Artru and G. B. Yodh, Phys. Lett. 40B, 43 (1972).
13. R. Hofstadter and H. R. Collard, Nuclear radii determined by electron scattering, p.21, Landolt-Bornstein, New series, I/2 Springer Verlag (1967).

Table I. PRODUCTION CROSS SECTIONS AND ERRORS (mb).

BEAM	ENERGY	SECONDARY			TARGET						
		Z_F	A_F	Y_B^F	H	Be	C	Al	Cu	Ag	Pb
^{16}O	2.10 GeV/n	1	1 [b]	50.7± 3.1	37.2± 6.8		96.5± 6.2				
		1	2	222.± 11.	152.± 23.	417.± 37.	406.± 36.		602.± 73.	752.± 97.	945.±154.
		1	3	78.3± 5.2	54.9±10.7		151.± 11.				
		2	3	72.8± 3.6	50.2± 5.7	152.± 9.	136.± 8.				
		2	4	257.± 13.	221.± 20.	501.± 45.	474.± 42.		748.± 80.	825.± 90.	882.±104.
		2	6	1.02± .10	.728±.204		2.00± .21				
		3	6	17.5± .9	13.2± 2.4	33.5± 2.7	35.9± 2.9		61.2± 7.9	49.4± 8.5	56.0±13.4
		3	7	13.5± .7	11.1± 1.3	27.0± 1.3	26.3± 1.3	34.8± 1.8	38.7± 2.9	39.8± 3.5	39.7± 4.3
		3	8	1.23± .08	.731±.169		2.50± .18		3.63± .47		
		3	9	.281±.033	.341±.078		.509±.067				
		4	7	11.4± .6	10.1± 1.2	22.0± 1.1	22.3± 1.1		32.0± 2.5	36.4± 3.2	43.3± 6.4
		4	9	4.68± .23	4.17± .55	9.79± .50	9.06± .51	11.2± .7	12.3± 1.1	13.8± 1.5	15.3± 2.1
		4	10	2.01± .10	2.05± .31	3.92± .27	3.98± .30		6.51± .86	5.65± .77	6.80±1.14
		4	11	.099±.014	.082±.031		.194±.033		.304±.127		
		4	12	.022±.008	.045±.020		.033±.016				
		5	8	.707±.039	.580±.083	1.53± .12	1.38± .13		1.38± .34		
		5	10	10.1± .5	8.86±1.66	19.1± 1.5	20.3± 1.6		35.2± 5.5	26.6± 6.3	35.2±11.3
		5	11	13.6± .7	15.4± 1.5	27.5± 1.4	25.9± 1.3	31.0± 1.6	35.8± 2.9	43.6± 3.9	52.8± 5.9
		5	12	1.33± .07	1.45± .17	2.75± .15	2.44± .15	3.61± .24	2.98± .38	4.04± .58	3.98± .75
		5	13	.248±.014	.314±.050	.502±.043	.437±.045		.820±.169	.651±.280	.699±.436
		6	9	.217±.040	.208±.077		.408±.086				
		6	10	1.43± .07	1.83± .21	2.81± .17	2.51± .16		4.45± .52	4.18±1.22	7.21±1.40
		6	11	10.2± .5	11.0± 1.1	21.0± 1.0	18.5± .9		27.0± 2.5	37.8± 3.8	36.9± 5.7
		6	12	32.3± 1.6	32.3± 4.8	60.8± 4.9	65.1± 5.2		91.5±14.4	104.± 10.	126.± 25.
		6	13	14.0± .7	17.8± 1.7	28.6± 1.4	27.7± 1.4	31.4± 2.0	35.8± 3.7	39.4± 5.1	45.4± 8.3
		6	14	2.65± .13	3.69± .38	5.21± .30	4.71± .31	6.29± .46	7.76± .92	7.51±1.30	12.3± 2.2
		6	15	.023±.004	.016±.011	.052±.010	.040±.013		.113±.079		
		7	12	.333±.020	.397±.069	.655±.055	.731±.071		.416±.179	1.11± .34	
		7	13	4.27± .21	4.49± .46	8.01± .40	8.06± .42		14.7± 1.5	18.6± 2.2	17.0± 3.1
		7	14	24.0± 1.2	31.0± 3.2	49.5± 4.0	41.8± 3.3		72.4±13.6	68.3±23.3	71.2±22.5
		7	15	29.1± 1.5	34.2± 3.3	54.1± 2.7	54.2± 2.9	66.0± 4.3	98.2± 9.6	121.± 15.	202.± 26.
		7	16	.039±.006	.019 a	.054±.016	.129±.023	.100±.034		.386±.151	.061 a
		8	13	.143±.012	.166±.035	.318±.035	.221±.035		.525±.167		
		8	14	.809±.040	.751±.120	1.60± .10	1.67± .12		2.14± .42	2.20± .58	2.80±1.52
		8	15	23.0± 1.2	27.3± 2.6	43.0± 2.1	42.9± 2.3		74.0± 7.8	99.2±12.6	135.± 22.
^{12}C	2.10 GeV/n	1	1 [b]	37.7± 1.9	24.1± 4.1	71.7± 4.2	70.0± 4.2	86.3± 5.7	112.± 9.	131.± 12.	171.± 18.
		1	2	173.± 9.	105.± 15.	329.± 30.	314.± 28.	411.± 37.	543.± 58.	690.± 78.	715.±124.
		1	3	69.0± 3.4	52.7±10.3	134.± 10.	129.± 11.	158.± 14.	198.± 24.	237.± 32.	321.± 52.
		2	3	66.9± 3.3	51.5± 4.5	128.± 7.	125.± 7.	152.± 9.	192.± 13.	227.± 16.	264.± 22.
		2	4	198.± 10.	171.± 15.	383.± 34.	373.± 33.	451.± 40.	553.± 59.	616.± 67.	728.± 85.
		2	6	1.19± .06	.906±.214	2.54± .25	2.21± .22	2.82± .27	3.21± .47	3.54±1.12	4.21±1.10
		3	6	16.0± .8	13.9± 1.5	33.1± 2.6	30.0± 2.4	36.3± 2.9	47.3± 4.5	46.1± 5.6	60.0± 8.5
		3	7	11.6± .6	11.0± 1.0	22.8± 1.1	21.5± 1.1	27.3± 1.4	31.9± 2.3	40.3± 3.3	45.9± 4.6
		3	8	1.19± .06	1.13± .16	2.52± .16	2.18± .15	2.79± .23	3.89± .47	3.27± .53	3.40± .82
		3	9	.432±.023	.406±.083	.919±.078	.851±.082	.883±.117	1.38± .36	1.20± .33	1.43± .53
		4	7	10.5± .5	9.49± .99	18.9± .9	18.6± .9	25.8± 1.3	33.7± 2.3	41.2± 3.3	47.9± 4.9
		4	9	5.62± .28	5.92± .54	11.0± .5	10.6± .5	12.7± .7	16.1± 1.3	18.6± 1.7	22.5± 2.6
		4	10	3.01± .15	3.42± .35	5.97± .31	5.81± .29	7.02± .40	8.57± .70	8.81± .91	9.97±1.40
		4	11	.009±.004		.018±.008					
		5	8	.756±.038	.468±.110	1.48± .09	1.72± .13	1.76± .14	1.85± .33	1.96± .40	3.69± .76
		5	10	16.5± .9	16.9± 3.0	31.1± 2.6	35.1± 3.4	36.3± 4.8	43.7± 9.8	64.6±17.4	73.8±24.5
		5	11	28.4± 1.4	30.9± 3.4	53.2± 2.9	53.8± 2.7	65.2± 4.7	84.8± 9.0	109.± 13.	155.± 23.
		5	12	.058±.004	.059±.010	.141±.018	.104±.010	.144±.033	.124±.075		.110 a
		6	9	.257±.017	.378±.074	.536±.056	.539±.066	.497±.086	.924±.172	.528±.269	1.56± .57
		6	10	2.13± .11	2.38± .24	4.20± .21	4.11± .22	4.99± .34	5.38± .55	7.03± .88	7.82±1.47
		6	11	25.5± 1.3	26.1± 2.4	46.7± 2.3	46.5± 2.3	59.5± 3.1	81.3± 6.3	102.± 10.	149.± 17.
		7	12	.035±.004	.034±.010	.058±.011	.079±.011			.240±.095	
^{12}C	1.05 GeV/n	1	1 [b]	10.2± .5	7.03±1.50	20.2± 1.4	18.8± 1.6	24.6± 2.1	26.4± 3.7	35.9± 5.2	48.7± 8.2
		1	2	168.± 8.	125.± 16.	301.± 27.	292.± 26.	413.± 37.	485.± 52.	698.± 82.	823.±145.
		1	3	63.6± 3.2		124.± 7.	118.± 7.	149.± 9.	219.± 19.		
		2	3	70.8± 3.5	46.4± 5.1	134.± 7.	135.± 8.	161.± 9.	209.± 14.	237.± 17.	321.± 26.
		2	4	214.± 11.	185.± 19.	422.± 30.	404.± 36.	488.± 44.	568.± 61.	727.± 79.	749.±113.
		2	6	.996±.054	.942±.188	2.09± .17	1.83± .19	2.00± .29	3.01± .68	3.61±1.38	7.27±2.67
		3	6	12.5± .6	11.5± 2.2	24.8± 2.0	27.1± 2.2	24.9± 2.9	33.1± 6.0	38.1± 7.6	50.5±13.1
		3	7	11.8± .6	10.4± .8	23.4± 1.2	21.5± 1.1	28.5± 1.4	32.6± 1.9	42.1± 3.4	45.2± 4.8
		3	8	1.18± .06	.770±.139	2.36± .14	2.40± .18	2.87± .27	3.99± .70	2.84±1.22	4.96±1.64
		3	9	.399±.026	.399±.093	.755±.078	.873±.096	.818±.159	1.05± .38	1.15± .49	1.76± .81
		4	7	8.93± .45	8.45± .81	17.8± .9	18.6± .9	19.9± 1.1	25.0± 1.9	21.6± 2.7	37.8± 4.7
		4	9	5.71± .29	5.13± .54	11.6± .7	10.7± .5	13.9± .9	14.3± 1.2	23.7± 2.7	22.2± 3.7
		4	10	2.74± .14	3.41± .35	5.08± .30	5.34± .29	6.49± .48	7.69± .61	8.43±1.19	10.9± 1.8
		4	11	.009 a		.018±.015					
		5	8	.749±.037	.600±.093	1.55± .08	1.43± .10	1.73± .16	2.29± .32	1.78± .38	2.70± .68
		5	10	14.5± .7	20.2± 2.5	28.8± 2.3	27.9± 2.2	30.4± 3.5	36.4± 9.9	43.1±12.4	50.9±10.2
		5	11	26.8± 1.3	29.3± 2.7	50.7± 3.2	48.6± 2.4	64.5± 5.3	80.1± 7.9	110.± 15.	149.± 25.
		5	12	.052±.005	.050±.013	.093±.017	.099±.013	.178±.046	.149±.047		.233 a
		6	9	.240±.016	.285±.061	.419±.048	.480±.060	.602±.100	.665±.183	1.19± .30	
		6	10	2.25± .11	2.52± .28	4.02± .23	4.44± .24	5.06± .37	7.53± .70	7.69±1.03	10.9± 1.7
		6	11	24.2± 1.2	25.0± 3.0	44.7± 2.6	44.7± 2.8	57.8± 3.9	78.1± 8.1	98.4±13.3	128.± 22.
		7	12	.014±.005	.053 a	.022±.011	.051 a	.069±.030			
TARGET FACTOR (Y_T)				1.00	.66+.028A_F	1.99± .02	1.92± .02	2.35± .03	2.81± .05	3.15± .07	3.72± .09

a FACTOR OF 2 ESTIMATE

b PROTON PRODUCTION WITHIN 12.5 MR OF 0 DEGREES.

Figure Captions

Figure 1. The cross sections for B+T → F + - can be expressed as $\sigma_{BT}^{F}=\gamma_{B}^{F}\gamma_{T}$, where γ_T is the target factor. Plotted are the mean target factors versus the target mass A_T (amu) for all cross sections given in Table I. The error bars represent the error-weighted standard deviations and reflect the distribution of errors in the individual cross sections σ_{BT}^{F}. The mean errors for γ_T are approximately the dot size. The computed values of γ_T using the empirical fit are given by the symbol X. Physical parameters in the empirical expression for γ_T are r_T, the half-density charge radius and t, the charge-skin thickness of the target nuclei (see Ref. 13). The line superimposed on the data points is an approximation for $\gamma_T=A_T^{\frac{1}{4}}$.

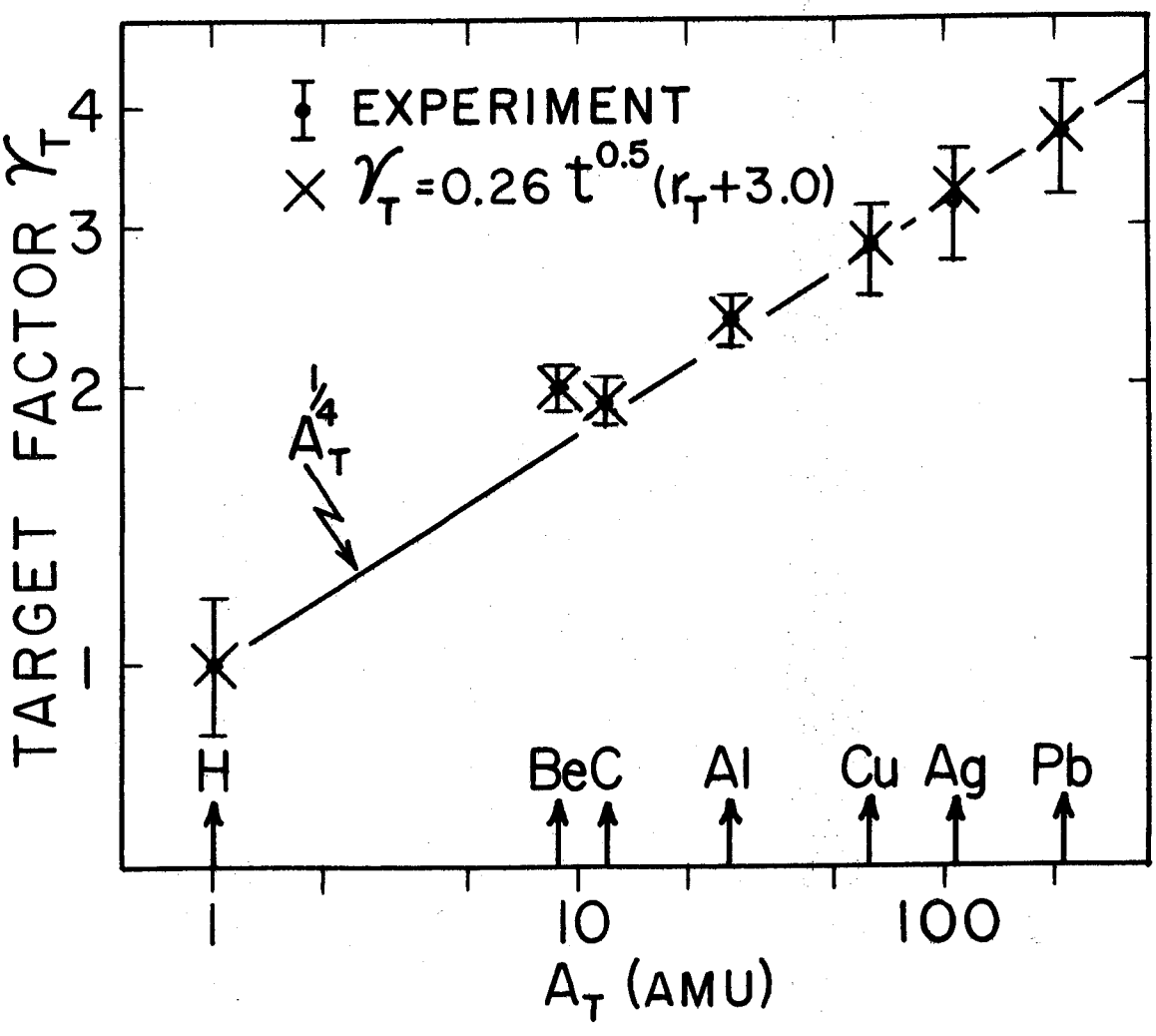
EXPERIMENT
$\gamma_T = 0.26\, t^{0.5}(r_T + 3.0)$
TARGET FACTOR γ_T
$A_T^{1/4}$
H
BeC
Al
Cu
Ag
Pb
1
10
100
A_T (AMU)
XBL 751-130

Fig. 1